

# Measurements of $\phi$ meson and $\Xi^-$ hyperon production in Au+Au collisions at $\sqrt{s_{NN}} = 3$ GeV from STAR experiment

Yingjie Zhou<sup>1\*</sup> (for the STAR Collaboration)

<sup>1</sup> Key Laboratory of Quark and Lepton Physics (MOE) and Institution of Particle Physics, Central China Normal University, Wuhan 430079, P. R. China

\* yingjiezhou@mails.cnu.edu.cn

October 27, 2021

*50th International Symposium on Multiparticle Dynamics  
(ISMD2021)*

12-16 July 2021

doi:10.21468/SciPostPhysProc.?



## Abstract

In this proceedings, we present our first measurements of  $\phi$  meson and  $\Xi^-$  hyperon production in Au+Au collisions at  $\sqrt{s_{NN}} = 3$  GeV. Various models including thermal and transport model calculations are compared to data, these results imply that the matter produced in the 3 GeV Au+Au collisions is considerably different from that at higher energies.

## Contents

<b>1</b>	<b>Introduction</b>	<b>1</b>
<b>2</b>	<b>Experiment</b>	<b>2</b>
<b>3</b>	<b>Particle yields</b>	<b>2</b>
<b>4</b>	<b>Yield ratios</b>	<b>4</b>
<b>5</b>	<b>Conclusion</b>	<b>5</b>
<b>References</b>		<b>5</b>

## 1 Introduction

The main goal of the STAR experiment is to study the properties of QCD matter at extreme conditions, high temperature and/or high density, by colliding heavy ions at ultra-relativistic speed. The yields and particle ratios of strange hadrons provide important information about the particle production mechanisms in these collisions. The RHIC Beam Energy Scan program covers a wide range of energies to explore the transition from a hadronic dominated phase to

24 a partonic dominated one. Of particular interest is the high baryon density region which is  
 25 accessible through the STAR fixed-target program, which has extended the energy reach from  
 26  $\sqrt{s_{NN}} = 13.7$  GeV down to 3.0 GeV.

27 Statistical thermal models have often been used to characterize the thermal properties  
 28 of the produced media. In low energies, the strangeness production is rare, therefore it has  
 29 been argued that strangeness number needs to be conserved locally on an event-by-event basis  
 30 described by the Canonical Ensemble (CE), which leads to a reduction in the yields of hadrons  
 31 with non-zero strangeness number [1–3], but not for the  $\phi$  meson with zero net strangeness  
 32 number ( $S=0$ ). The  $\phi/K^-$  ratio is expected to increase with decreasing collision energy in  
 33 models using the CE treatment for strangeness, opposite to the trend in the Grand Canonical  
 34 Ensemble (GCE) treatment. The canonical suppression power for  $\Xi^-$  ( $S=2$ ) is even larger than  
 35 for  $K^-$  ( $S=1$ ). The  $\phi/K^-$  and  $\phi/\Xi^-$  ratios offer a unique test to scrutinize thermodynamic  
 36 properties of strange quarks in the hot and/or dense QCD environment [4].

37 In this proceedings, the first measurements of  $\phi$  meson and  $\Xi^-$  hyperon production as well  
 38 as the ratios of  $\phi/K^-$  and  $\phi/\Xi^-$  in Au+Au collisions at  $\sqrt{s_{NN}} = 3$  GeV will be presented.

## 39 2 Experiment

40 The dataset used in this analysis consists of Au+Au collisions at  $\sqrt{s_{NN}} = 3$  GeV collected by the  
 41 STAR experiment under the fixed target (FXT) configuration in the year of 2018. The single  
 42 beam was provided by RHIC with total energy equal to 3.85 GeV/nucleon. The thickness of the  
 43 gold target is about 0.25 mm, corresponding to a 1% interaction probability to minimize the  
 44 pileup and energy loss effect in target. The target is located at 200 cm to the west of the center  
 45 of the STAR detector, it is installed inside the vacuum pipe, 2 cm below the center of the beam  
 46 axis. The minimum bias (MB) trigger condition is provided by the Beam-Beam Counters (BBC).  
 47 Tracking and particle identification (PID) are done using the energy loss ( $dE/dx$ ) information  
 48 from Time Projection Chamber (TPC) and time of flight ( $1/\beta$ ) information from Time of Flight  
 49 (TOF). In total, approximately  $2.6 \times 10^8$  MB triggered events are used in this analysis.

## 50 3 Particle yields

51 Reconstruction of short lived particles  $\Xi^- \rightarrow \Lambda + \pi^-$  is performed using the KF Particle Finder  
 52 package based on the Kalman Filter method [5]. Those combinatorial backgrounds are ob-  
 53 tained by rotating daughter tracks. The  $\phi$  mesons are reconstructed through the hadronic  
 54 decay channel,  $\phi \rightarrow K^+ + K^-$ , where combinatorial background is estimated using the mixed  
 55 event technique. The reconstructed  $\Xi^-$  and  $\phi$  candidates are shown in Fig. 1 (a,b). The num-  
 56 ber of signal counts is extracted using a bin counting method, and is shown as a function of  
 57  $p_T - y_{cm}$  in Fig. 1 (c,d). Good mid-rapidity coverage is attained in the  $\sqrt{s_{NN}} = 3$  GeV Au+Au  
 58 collisions.

59 The numbers of  $K^-$ ,  $\phi$  and  $\Xi^-$  counts in the data are extracted as a function of  $m_T - m_0$  in  
 60 different rapidity and centrality selections. The raw signal counts in each  $m_T - m_0$  interval are  
 61 subsequently corrected by the acceptance and reconstruction efficiency estimated via GEANT3  
 62 [6]. The corrected  $K^-$ ,  $\phi$ , and  $\Xi^-$   $dN/dm_T$  are all well described by  $m_T$  exponential functions.  
 63 The  $m_T$  and rapidity differential yield of  $K^-$  and  $\phi$  meson in 0-10% centrality collisions are  
 64 shown in Fig. 2.

65 We considered three sources of systematic uncertainties, arising from (1) imperfect de-  
 66 scription of topological variables in the simulations, (2) the tracking efficiency of the TPC,  
 67 and (3) the background subtraction method. Their contributions are estimated by varying

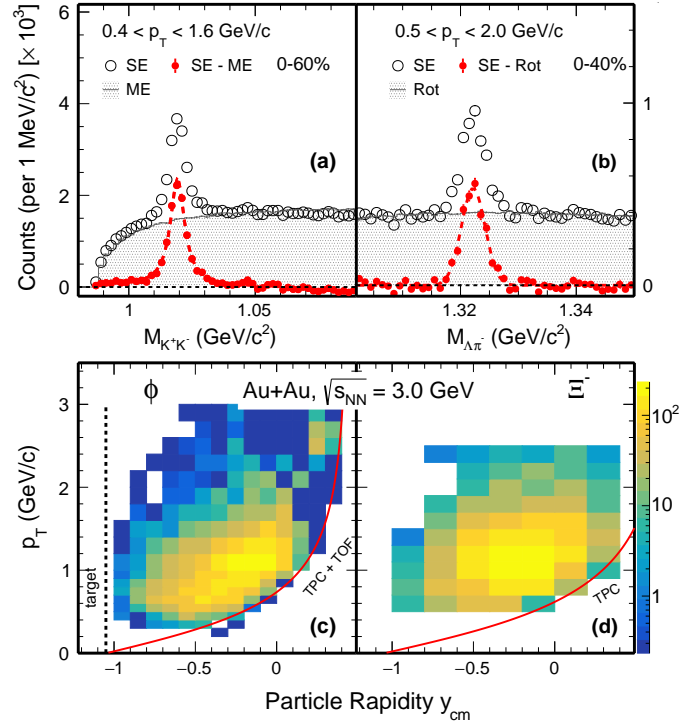


Figure 1: Invariant mass distributions of (a)  $K^+K^-$  and (b)  $\Lambda\pi^-$  pairs reconstructed from data are shown on the top. The grey shaded histogram represents the normalized mixed-event (rotating daughters for  $\Xi^-$ ) unlike-sign distribution that is used to estimate the combinatorial background. The transverse momentum ( $p_T$ ) versus the rapidity ( $y_{cm}$ ) for reconstructed (c)  $\phi$  and (d)  $\Xi^-$  are shown on the bottom.

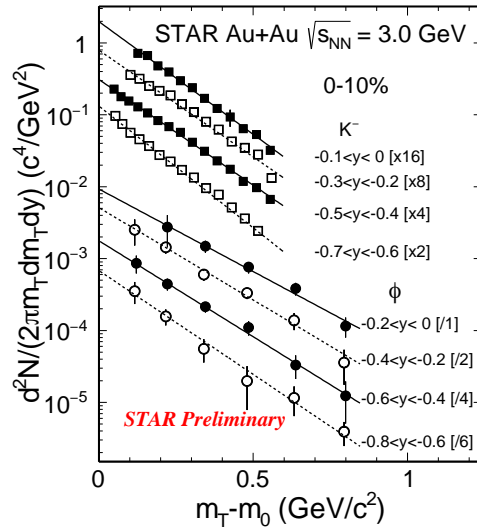


Figure 2:  $m_T$  spectra for  $K^-$  and  $\phi$  in 0-10% Au+Au collisions at  $\sqrt{s_{NN}} = 3$  GeV in different rapidity selections. The solid and dashed black lines represent fits using the  $m_T$  exponential function to the data points.

69 ground subtraction method. These uncertainties are assumed to be uncorrelated and added  
70 in quadrature.

71 To estimate the  $p_T$  integrated yield, the data are extrapolated down to  $p_T = 0$ . Besides the  
72 aforementioned systematic uncertainties, uncertainties from extrapolation to the unmeasured  
73 regions are considered, i.e. different functional forms are used for the extrapolation to estimate  
74 this uncertainty. The  $p_T$  integrated  $dN/dy$  as a function of rapidity are shown in Fig. 3. Solid  
75 curves depict Gaussian function fits to the data points with the centroid parameter fixed to  
76 zero. They are used to extrapolate to the unmeasured rapidity region for calculating total  
multiplicities.

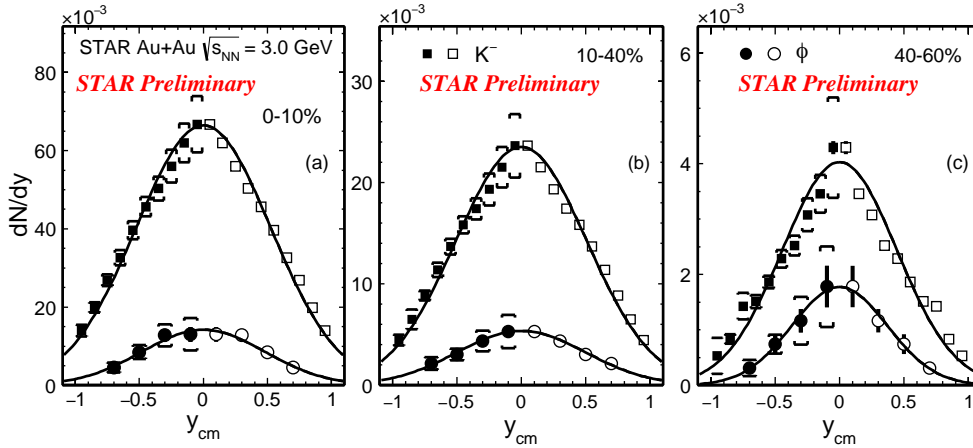


Figure 3: Rapidity distributions of  $K^-$  and  $\phi$  meson for various centrality regions, solid symbols are measured data, open ones are reflection. Yields obtained from integrating fit functions to the  $m_T$  spectra are fit with a Gaussian function.

77

## 78 4 Yield ratios

79 Figure 4 shows the  $\phi/K^-$  (left) and  $\phi/\Xi^-$  (right) ratios from our measurements in differ-  
80 ent centralities as a function of  $\sqrt{s_{NN}}$ . The measured  $\phi/K^-$  and  $\phi/\Xi^-$  ratios at 3 GeV are  
81 slightly higher than the values at high energies for  $\sqrt{s_{NN}} \geq 5$  GeV. There is a hint that both  
82 the measured  $\phi/K^-$  and  $\phi/\Xi^-$  ratios in mid-central collisions are larger than those in central  
83 collisions, and this needs further statistics to systematically study the centrality dependence in  
84 detail. The GCE underestimates our data with  $\sim 5\sigma$  effect for  $\phi/K^-$  and  $\sim 4\sigma$  effect for  $\phi/\Xi^-$ ,  
85 while the CE calculation with strangeness correlation length ( $r_c$ )  $\sim 3.2$  fm can reasonably de-  
86 scribe our measurements. The precise determination of the thermal parameters (including  
87  $T_{ch}$ ,  $\mu_B$  and  $r_c$ ) needs a global thermal model fit with all the particle yields at 3 GeV. The  
88 modified transport models (UrQMD and SMASH) including high mass resonances decay to  $\phi$   
89 and  $\Xi^-$  can also reasonably describe the data at low energies [7–14]. In the Au+Au collisions  
90 at 3 GeV, the observed strangeness production mechanism may be different from that at high  
91 energies, and this may indicate a change of Equation of State (EoS) at this low energy.

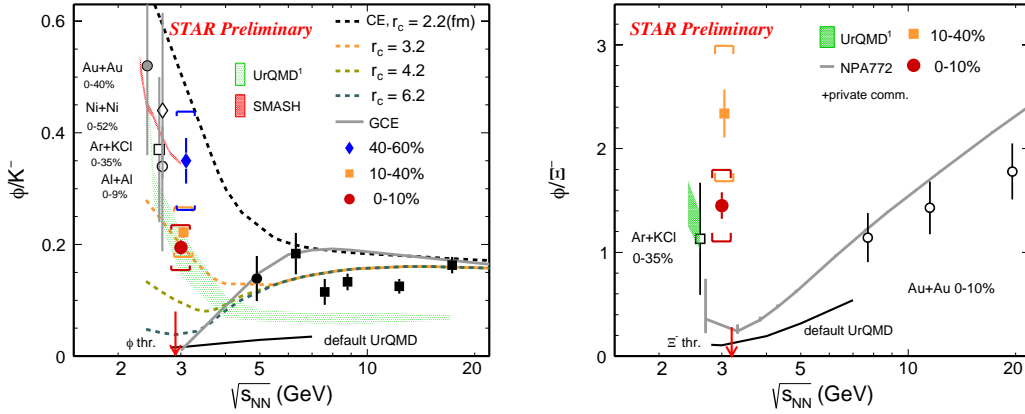


Figure 4:  $\phi/K^-$  (left) and  $\phi/\Xi^-$  (right) ratios as a function of  $\sqrt{s_{NN}}$ . The solid color markers show the measurements at 3 GeV from different centrality bins with vertical lines for statistical and bracket symbols for systematic errors, while other markers are used for data from various other energies and/or collision systems [7–14].

## 92 5 Conclusion

93 We report the systematic measurements of  $K^-$ ,  $\phi$  meson and  $\Xi^-$  hyperon production yields  
 94 and the  $\phi/K^-$ ,  $\phi/\Xi^-$  ratios in Au+Au collisions at  $\sqrt{s_{NN}} = 3$  GeV with the STAR experiment  
 95 at RHIC. The measured  $\phi/K^-$  ratio is significantly larger than the statistical model prediction  
 96 based on GCE in the 0–10% central collisions. Both the results of  $\phi/K^-$  and  $\phi/\Xi^-$  ratios  
 97 favor the Canonical Ensemble model for strangeness production in such collisions. Transport  
 98 models, including the resonance decays, could reasonably describe our measured  $\phi/K^-$  ratio  
 99 at 3 GeV and the increasing trend of  $\phi/\Xi^-$  at lower energies. These results suggest a significant  
 100 change in the strangeness production at  $\sqrt{s_{NN}} = 3$  GeV compared to higher collision energies,  
 101 providing new insights towards the understanding of the QCD medium properties at high  
 102 baryon density [15].

## 103 Acknowledgements

104 This work was supported in part by the National Key Research and Development Program  
 105 of China under Grant No. 2020YFE0202002, and the Fundamental Research Funds for the  
 106 Central Universities under Grant No. CCNU20TS005.

## 107 References

- 108 [1] J. Rafelski and M. Danos, *The importance of the reaction volume in hadronic col-*  
 109 *lisions*, Physics Letters B **97**(2), 279 (1980), doi:[https://doi.org/10.1016/0370-](https://doi.org/10.1016/0370-2693(80)90601-2)  
 110 [2693\(80\)90601-2](https://doi.org/10.1016/0370-2693(80)90601-2).  
 111 [2] J. Rafelski and J. Letessier, *Importance of reaction volume in hadronic collisions: canonical*  
 112 *enhancement*, Journal of Physics G: Nuclear and Particle Physics **28**(7), 1819 (2002),  
 113 doi:[10.1088/0954-3899/28/7/336](https://doi.org/10.1088/0954-3899/28/7/336).

- 114 [3] K. Redlich and A. Tounsi, *Strangeness enhancement and energy dependence in heavy ion*  
115 *collisions*, Eur. Phys. J. C **24**, 589 (2002), doi:[10.1007/s10052-002-0983-1](https://doi.org/10.1007/s10052-002-0983-1).
- 116 [4] M. S. Abdallah *et al.*, *Probing Strangeness Canonical Ensemble with  $K^-$ ,  $\phi(1020)$  and  $\Xi^-$*   
117 *Production in Au+Au Collisions at  $\sqrt{s_{NN}} = 3$  GeV* (2021), [2108.00924](https://arxiv.org/abs/2108.00924).
- 118 [5] I. Kisel, *Event Topology Reconstruction in the CBM Experiment*, J. Phys. Conf. Ser. **1070**(1),  
119 012015 (2018), doi:[10.1088/1742-6596/1070/1/012015](https://doi.org/10.1088/1742-6596/1070/1/012015).
- 120 [6] R. Brun, A. McPherson, P. Zancarini, M. Maire and F. Bruyant, *Geant 3: user's guide geant*  
121 *3.10, geant 3.11*, Tech. rep., CERN (1987).
- 122 [7] B. Back, R. Betts, J. Chang, W. Chang, C. Chi, Y. Chu, J. Cumming, J. Dunlop, W. Eldredge,  
123 S. Fung *et al.*, *Production of  $\phi$  mesons in Au+Au collisions at 11.7 A GeV/c*, Physical  
124 Review C **69**(5), 054901 (2004), doi:[10.1103/PhysRevC.69.054901](https://doi.org/10.1103/PhysRevC.69.054901).
- 125 [8] C. Alt *et al.*, *Energy dependence of phi meson production in central Pb+Pb collisions at  $\sqrt{s_{NN}}$*   
126 *= 6 to 17 GeV*, Phys. Rev. C **78**, 044907 (2008), doi:[10.1103/PhysRevC.78.044907](https://doi.org/10.1103/PhysRevC.78.044907),  
127 [0806.1937](https://arxiv.org/abs/0806.1937).
- 128 [9] J. Adam *et al.*, *Strange hadron production in Au+Au collisions at  $\sqrt{s_{NN}} = 7.7,$*   
129 *11.5, 19.6, 27 and 39 GeV*, Phys. Rev. C **102**(3), 034909 (2020),  
130 doi:[10.1103/PhysRevC.102.034909](https://doi.org/10.1103/PhysRevC.102.034909), [1906.03732](https://arxiv.org/abs/1906.03732).
- 131 [10] P. Gasik, K. Piasecki, N. Herrmann, Y. Leifels, T. Matulewicz, A. Andronic, R. Averbeck,  
132 V. Barret, Z. Basrak, N. Bastid *et al.*, *Strange meson production in Al+Al collisions at 1.9 A*  
133 *GeV*, The European Physical Journal A **52**(6), 1 (2016), doi:[10.1140/epja/i2016-16177-](https://doi.org/10.1140/epja/i2016-16177-y)  
134 [y](https://doi.org/10.1140/epja/i2016-16177-y).
- 135 [11] K. Piasecki, N. Herrmann, R. Averbeck, A. Andronic, V. Barret, Z. Basrak, N. Bastid,  
136 M. Benabderrahmane, M. Berger, P. Buehler *et al.*, *Influence of  $\phi$  mesons on negative*  
137 *kaons in Ni+Ni collisions at 1.91 A GeV beam energy*, Physical Review C **91**(5), 054904  
138 (2015), doi:[10.1103/PhysRevC.91.054904](https://doi.org/10.1103/PhysRevC.91.054904).
- 139 [12] G. Agakishiev *et al.*,  *$\phi$  decay: A Relevant source for K- production at SIS energies?*, Phys.  
140 Rev. C **80**, 025209 (2009), doi:[10.1103/PhysRevC.80.025209](https://doi.org/10.1103/PhysRevC.80.025209), [0902.3487](https://arxiv.org/abs/0902.3487).
- 141 [13] J. Adamczewski-Musch *et al.*, *Deep sub-threshold  $\phi$  production in Au+Au collisions*, Phys.  
142 Lett. B **778**, 403 (2018), doi:[10.1016/j.physletb.2018.01.048](https://doi.org/10.1016/j.physletb.2018.01.048), [1703.08418](https://arxiv.org/abs/1703.08418).
- 143 [14] G. Agakishiev *et al.*, *Deep sub-threshold  $\Xi^-$  production in Ar+KCl reactions at 1.76A-GeV*,  
144 Phys. Rev. Lett. **103**, 132301 (2009), doi:[10.1103/PhysRevLett.103.132301](https://doi.org/10.1103/PhysRevLett.103.132301), [0907.3582](https://arxiv.org/abs/0907.3582).
- 145 [15] Ko, Che Ming, *Theoretical perspective on strangeness production*, EPJ Web Conf. **171**,  
146 03002 (2018), doi:[10.1051/epjconf/201817103002](https://doi.org/10.1051/epjconf/201817103002).